

ARTICLE

Updated Trewartha climate classification with four climate change scenarios

Aleksandar Valjarević¹  | Miško Milanović¹ | Ismail Gultepe^{2,3,4} | Dejan Filipović¹ | Tin Lukić⁵

¹Faculty of Geography, Department of Geospatial and Environmental Science, University of Belgrade, Belgrade, Serbia

²Meteorological Research Division, ECCC, Toronto, Ontario, Canada

³Engineering and Applied Science, Ontario Tech University, Oshawa, Ontario, Canada

⁴Faculty of Engineering, Istinye University, Istanbul, Turkey

⁵Department of Geography, Tourism and Hotel Management, Faculty of Sciences, University of Novi Sad, Novi Sad, Serbia

Correspondence

Aleksandar Valjarević, Faculty of Geography, Department of Geospatial and Environmental Science, University of Belgrade, Belgrade, Serbia.

Email: aleksandar.valjarevic@gef.bg.ac.rs

Abstract

The Updated Trewartha climate classification (TWCC) at global level shows the changes that are expected as a consequence of global temperature increase and imbalance of precipitation. This type of classification is more precise than the Köppen climate classification. Predictions included the increase in global temperature (T in $^{\circ}\text{C}$) and change in the amount of precipitation (PA in mm). Two climate models MIROC6 and IPSL-CM6A- LR were used, along with 4261 meteorological stations from which the data on temperature and precipitation were taken. These climate models were used because they represent the most extreme models in the CMIP6 database. Four scenarios of climate change and their territories were analysed in accordance with the TWCC classification. Four scenarios of representative concentration pathway (RCP) by 2.6, 4.5, 6.0 and 8.5 W/m^2 follow the increase of temperature between 0.3°C and 4.3°C in relation to precipitation and are being analysed for the periods 2021–2040, 2041–2060, 2061–2080 and 2081–2100. The biggest extremes are shown in the last grid for the period 2081–2100, reflecting the increase of T up to 4.3°C . With the help of GIS (geographical information systems) and spatial analyses, it is possible to estimate the changes in climate zones as well as their movement. Australia and South East Asia will suffer the biggest changes of biomes, followed by South America and North America. Climate belts to undergo the biggest change due to such temperature according to TWCC are Ar, Am, Aw and BS, BW, E, Ft and Fi. The Antarctic will lose 11.5% of the territory under Fi and Ft climates within the period between 2081 and 2100. The conclusion is that the climates BW, Bwh and Bwk, which represent the deserts, will increase by 119.8% with the increase of T by 4.3°C .

KEYWORDS

climate scenarios, GIS, IPSL-CM6A- LR, MIROC6, updated Trewartha climate classification

1 | INTRODUCTION

The Köppen climate classification (1884) has been the most widely used system for determining climatic patterns (Köppen, 1923, 1931). This climate system uses mean monthly and annual values of T and PA and recognises five main climate groups, each marked by a capital letter. The Köppen climate classification is based on dominant vegetation types since most vegetation types respond directly to climatic inputs. This climate classification has been widely used lately and updated and improved territories of this classification have been provided (Kottek et al., 2006; Peel et al., 2007). The Trewartha climate classification presents the revised Köppen climate classification. As outlined by De Castro et al. (2007), this approach represents and upgrades the original Köppen system and introduces various modifications corresponding to the identified boundaries of natural landscapes. Köppen observed and mapped the ecotone or transitional zones between two biomes. Using such criteria, this climate system identified five main climatic groups: A – tropical, B – arid, C – mesothermal or mid-latitude mild, D – micro-thermal or mid-latitude cold, E – polar. According to many authors, the Trewartha climate classification is a revised Köppen classification of the second and third order. The letters of second order changes are: f – constant moist and rainfall through all months of the year; m – Monsoon rain, short dry season; s – summer dry season; w – winter dry season, W or S – hot and dry year-round and average annual temperature > 18°C. The letter h is in the third order dividing W or S – cold and dry year-round average annual temperature < 18°C, n – the letter in the third order for frequent fog, with n' being infrequent fog with high humidity and low rainfall (Feng et al., 2012; Rohli & Vega, 2012).

The Trewartha classification system can therefore be useful for the analysis of small climatic areas with varying plant coverage (Lai et al., 2020). Later, the geographical distribution of plants in case of T increase between 2.0°C and 3.0°C was studied using the Köppen-Geiger (K-G) system which is very similar but not identical to the Trewartha classification system (Rohli et al., 2015). Their work concluded that the most significant change in the climatic distributions was identified in the subtropical and tropical belts in north and south-east Asia (Prentice et al., 1993). Another advantage of TWCC is better zonal characteristics between areas (Hanberry & Fraser, 2019). Therefore, land management conditions can be improved by the use of spatial mapping methods. For example, species distribution modelling (SDM) with a fine resolution of DEM (digital elevation model) with an accuracy of 10 m may be applied to different climatic regions with an assumed minimum error (Keane et al., 2020). The goal of the present work, using the updated Trewartha climate classification and climatic analysis, is to evaluate the changes in climate types for temperature increases between 0.3°C and 4.3°C for the period between 2021 and 2100. All the predictions were made with the help of two climate models, which follows the prognosis of RCP2.6, RCP4.5, RCP6 and RCP8.5. The first projection shows T increasing minimally by the end of the century, the second one presents a minor increase, the third one moderate, whereas the fourth one presents an extreme temperature increase. All continents included in this research were shown on maps, with temperature values from the Fifth IPCC or Assessment Report 5 created in 2014 (Robinson, 2020). Since the Antarctic was also included in the analyses, this research covers the whole of the Earth.

2 | DATA AND ANALYSIS

Climate predictions were made using global climate models (GCMs). In this research, we used MIROC6 (Shiogama et al., 2019) (Japan Agency for Marine-Earth Science and Technology) and IPSL-CM6A- LR (Institut Pierre-Simon Laplace) climate models with included CMIP6 database. The climate prediction models estimated future climate using mathematical and numerical equations. These climate models were used as they are the most extreme ones with a wide range of climate scenarios. The main reason was the possibility to estimate and predict CMIP6 ensemble in terms of hot/dry to warm/wet, thereby giving the widest possible range of Trewartha climate classification responses (Crowther et al., 2015; Richardson et al., 2007).

All climate models have two main parameters: temperature and precipitation. These parameters are also connected with the biomes on Earth. Carbon dioxide (CO₂) concentration per year is also one of the important state variables. This variable may be used for future predictions of climate on a global scale (Idso & Brazel, 1984; North, 2013; Shakun et al., 2012; Zelinka et al., 2020). In 1988, the World Meteorological Organisation founded the Intergovernmental Panel on Climate Change (IPCC) to observe climate changes and the volume of particles of carbon dioxide in the air. The data we downloaded are available at different spatial resolutions expressed as minutes or seconds and in degrees of longitude and latitude. These data have a resolution of 0.86 km². The data on future climate belongs to the Coupled Model Intercomparison Project (CMIP6) (Tatebe et al., 2019). The data used for this research may be divided into two groups. The first group is the data taken from 4261 meteorological stations worldwide, from which the basic grid was obtained

using interpolation and zonal statistical methods. The first grid is made up of data on precipitation, with the help of which, a precise interpolated map of precipitation was derived, covering the global scale (see Figure 1).

The updated and analysed TWCC climate properties showed changes in T and PA which were integrated into the grids. The position of world meteorological stations is important to check data availability and climate surface symmetry. The total number of surface meteorological stations was 4261 (<https://databasin.org/datasets>; Govindasamy et al., 2003).

The second grid represents the data on average temperatures globally. The second type of data represented a synthetic, already obtained grid of two climate models. This grid was later compared with the first basic grid obtained from the meteorological stations. The first type of grid was taken to provide symmetry to later defined biomes, which were derived from the synthetic grid of two climate models. The borders of biomes in the two scenarios were obtained using interpolation, numerical analysis and zonal statistical methods. Average temperatures and the distribution of precipitation were used only as a control grid. Two climate models, more precisely their grid, already contain projected data on temperature values and the amount of precipitation. The basic data on TWCC are given in Table 1.

Since the data from both grids of climate projections were given for the periods 2021–2040, 2041–2060, 2061–2080 and 2081–2100, we continued with the selection of the grid by employing a categorisation algorithm and data zonality. The first period is between 2021 and 2040; the second is from 2041 to 2060, the third is from 2061 to 2080 and the fourth is from 2081 to 2100. Both climate models were taken from the database DIVA-GIS (<https://pcmdi.llnl.gov/CMIP6/TermsOfUse/TermsOfUse6-1.html>). This database is available free of charge, and it contains nine climate models (Comes & Kadereit, 1998; Flannigan et al., 2000; Tatebe et al., 2019; Tokarska et al., 2020). To analyse biomes completely and with fewer errors, we downloaded the control DEM with a resolution of 1 km². This DEM for all the continents was downloaded from the official website of NASA National (Mwanukuzi, 2008). All TWCC climate belts are divided according to the surface into three dimensions with elevation included and coloured with matching colours.

3 | GIS AND SPATIAL ANALYSIS

As was previously mentioned, for this research on biomes distribution according to the TWCC, basic GIS methodologies and algorithms were used. Apart from these basic analyses, we also used advanced GIS to present spatial data more precisely. The basic GIS algorithms used were inverse distance weight (IDW), surface interpolation (SI), kriging (KR),

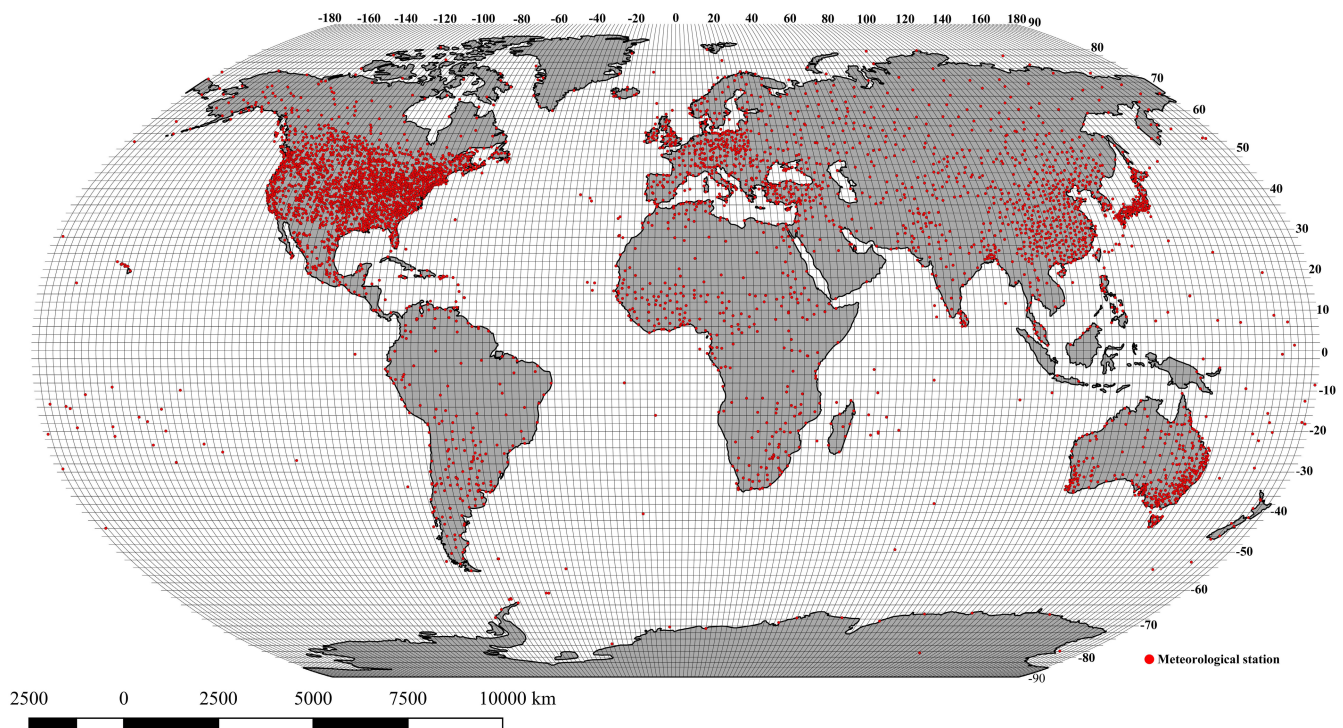


FIGURE 1 The number of meteorological stations used in the analysis was 4261. The stations had data on temperature and precipitation recorded between 1961 and 2000

and semi-kriging (SK). The advanced GIS methods used were zonal statistics (ZS), buffer (BF) and proximity (PR). In the methodology of spatial analysis, to get the grid with the dimension of elevation, we downloaded, processed and later analysed DEM by GIS tools (Daly et al., 2002; Hijmans et al., 2005; New et al., 2002; Thornton et al., 2007; Wilby & Wigley, 2002). GIS today represents a powerful tool, due to its accuracy, but also due to the fast processing of data. All GIS and spatial analyses were performed with the help of open code software SAGA 7.9.1 (Software for Automated Geoscientific Analyses), QGIS 3.18. (Quantum GIS). Due to the specificity of the architecture, we used DIVA GIS for the analysis of biomes. This software is the most suitable for climatological and bioclimatological analyses. Since the grid data are in raster format, by the process of turning the raster into a vector, i.e. vectorisation, we obtained dotted data for the whole grid (Smith et al., 2007). The purpose of turning surfaces into dots is to get more precise forms of biomes in terms of latitude and longitude in accordance with TWCC (Hansen et al., 2013). The total number of dots for the whole world was 81,048,142. The dots were distributed about the size of the continent, matching the biome. Since TWCC has 27 basic belts, the estimation was given for all of them in three future predictions. The last algorithm done in GIS is buffer. This algorithm sorts the data according to the climate values of the biome (temperature and precipitation) and sets the borders between them (Fick & Hijmans, 2017; Gotway et al., 1996; Orus et al., 2005; Timpano et al., 2011; Valjarević et al., 2018; Zabel et al., 2014). The main four maps present the climate properties for the four future periods: 2021–2040, 2041–2060, 2061–2080 and 2081–2100 (Belda et al., 2016). The overlap of the two grids was made possible by the proximity algorithm.

4 | RESULTS

The most precise grid was between 30°–75° of latitude and 30°–75° of south latitude. With the increase of latitude, the size of the grid increases as well, thus increasing the relative error. For this reason, the biggest error was in the continent Antarctic, going up to 0.5%, whereas the smallest error, due to the accuracy of the grid, was in South America, Africa, and a part of Asia, going up to 0.3%. The biggest errors were present in the territories close to the equator and varied between 1.5% and 2.0%. In general, the results showed that the biggest changes at the continental scale are expected after the increase of T by 3.1°C. The maximum change in climate belts is expected with the increase of T by 4.3°C.

5 | CHANGES OF TWCC AT CONTINENTAL SCALE

The biggest changes of TWCC will take place in the period 2081–2100, with the increase of T by 4.3°C. Australia and South East Asia will suffer the biggest changes of biome, followed by South America and North America. According to TWCC, climate belts to change the most at this temperature increase are Ar, Am, Aw and BS, BW, E, Ft and Fi. What is interesting is that the continent Antarctic shows a certain degree of resistance. In the period between 2081 and 2100, the continent will lose 11.5% of whole territory within Fi climate (see Figure 4). Climate types in the belts CW, CWa, CF, CFa, CFb, DC, DCs, DCsa, DCsb, DCwa and DCwb will undergo minor changes going from 5.2% to 12%.

With the increase of temperature by 2.5°C, biomes that belong to the Amazon basin will have 3.7% of changes in the total area of rainforest biomes. With the increase of 4.3°C, the Amazonian forests will lose 12.5% of their territory.

The forests in the moderate zones will suffer changes by 1.6%, 2.6%, 4.2% and 6.1%, respectively. Unlike forest biome, grassland will suffer the loss of 0.8% of the territory, with a temperature increase by 2.5°C, whereas with an increase by 4.3°C, the loss will be 2.2%.

Tundra will decrease globally by 0.5%, if the temperature increases by 2.3°C, while it will increase by 3.7% with a temperature increase by 4.3°C. The deserts will increase by 3.8% with an increase of T by 2.5°C, and 15.5% with an increase of T by 4.3°C (see Table 2, Figures 4 and 5 and the Appendix S1).

Table 2 and the Appendix S1 show the changes of certain climate types and their territories in percent. A change of 100% indicates a doubling of territory under a particular climate. Climate types Ar, Am and Aw, more precisely their territories, are the most sensitive to the T increase and unequal amount of precipitation. Australia and Asia will have a doubling of territories with this climate. These territories will increase by 56.1% following a T increase from 2.5°C to 4.3°C. Territories with climate types Ft and Fi, with the same increase of T will lose 39.3% of territory. North America will also have big increases of territory with climate types Ar and Am. Both territories will increase by 93.8%, thus doubling the territory under these climates, with a T increase by 2.5°C, i.e. 4.3°C.

TABLE 1 The Trewartha climate classification (Remedio et al., 2019)

Class	Type	Sub-type	Description	Rules
A			Tropical	Coollest month $>18^{\circ}\text{C}$
	Ar		Rainy tropical broadleaf forest	10 to 12 months wet
	Am		Tropical monsoonal forest	
	Aw		Tropical deciduous forests/woodland	Winter dry >2 dry months
B			Dry climates	Evaporation/precipitation
	BS		Semi-arid	Annual rainfall desert; limit of precipitation
		<i>BSh</i>	Tropical-subtropical scrubland	8 or more months $>10^{\circ}\text{C}$
		<i>BSk</i>	Temperate-boreal steppe	Less than 8 months $>10^{\circ}\text{C}$
	BW		Arid or desert	Annual rainfall $<$ desert limit of precipitation
		<i>BWh</i>	Tropical-subtropical desert	8 or more months $>10^{\circ}\text{C}$
		<i>BWk</i>	Temperate-cold desert	Less than 8 months $>10^{\circ}\text{C}$
C			Subtropical climates	8 to 12 months $>10^{\circ}\text{C}$
	Cw		Subtropical winter dry season	Winter dry season
		<i>CWa</i>	Mixed broadleaf deciduous and needleleaf forest	Warmest month $>22^{\circ}\text{C}$
		<i>CWb</i>	Needleleaf evergreen and broadleaf evergreen forest	Warmest month $<22^{\circ}\text{C}$
	Cf		Subtropical humid	Driest month >30 mm
		<i>CFa</i>	Needleleaf evergreen and broadleaf evergreen forests and evergreen broadleaf shrub understory	Warmest month $>22^{\circ}\text{C}$; no distinct dry season
		<i>CFb</i>	Needleleaf evergreen and deciduous forest	Warmest month $<22^{\circ}\text{C}$; no distinct dry season
D			Temperate climates	4 to 7 months $>10^{\circ}\text{C}$
	DC		Temperate continental climate	Coldest month $<0^{\circ}\text{C}$
	DCs		Summer dry season	Summer dry season
		<i>DCsa</i>	Mixed evergreen and deciduous forest	Warmest month $>22^{\circ}\text{C}$
		<i>DCsb</i>	Mixed evergreen and deciduous forest	Warmest month $<22^{\circ}\text{C}$
	DCw		Winter dry season	Winter dry season
		<i>DCwa</i>	Mixed deciduous and needleleaf evergreen forests	Warmest month $>22^{\circ}\text{C}$
		<i>DCwb</i>	Needleleaf evergreen forest	Warmest month $<22^{\circ}\text{C}$
	DCf		Humid continental	Driest month >30 mm

(Continues)

TABLE 1 (Continued)

Class	Type	Sub-type	Description	Rules
		DCfa	Mid-latitude grassland, broadleaf deciduous forests and woodlands, mixed evergreen and broadleaf forests	Warmest month $>22^{\circ}\text{C}$; no distinct dry season
		DCfb	Needleleaf evergreen and mixed needleleaf-deciduous forest	Warmest month $<22^{\circ}\text{C}$; no distinct dry season
E			Needleleaf deciduous forest and tundra woodland	1 to 3 months $>10^{\circ}\text{C}$
F	Ft		Polar Tundra, high altitude steppe	$0^{\circ}\text{C} \leq$ warmest month $<10^{\circ}\text{C}$
	Fi		Perpetual frost	All months $<0^{\circ}\text{C}$

TABLE 2 Changes of the climate types and their territories with the temperature increase by 4.3°C : – indicates decreasing values and + increasing values of areas in the period between 2081 and 2100

Territories of the same climate types Changing [%]	South America	North America	Africa	Europe	Asia	Australia	Antarctica
Ar	+81.2	+133.3	+59.8	0.0	+102.2	+112.1	0.0
Am	+40.3	+106.6	+15.5	0.0	+89.9	+344.4	0.0
Aw	+189.2	+9.5	+10.9	0.0	+41.2	+122.2	0.0
BS	+23.3	+23.4	+23.3	+153.1	+12.2	+11.7	0.0
BSh	+39.8	+11.2	+43.4	+72.1	+16.5	+28.8	0.0
BSk	+11.8	+5.7	+22.3	+18.6	+6.1	+5.1	0.0
BW	+20.0	+11.1	+7.1	0.0	+2.3	+20.9	0.0
BWh	+24.5	+25.5	+0.2	0.0	–34.4	–2.1	0.0
BWk	+10.9	+14.5	+25.6	0.0	+13.3	+23.5	0.0
CW	–10.9	+5.6	+4.9	0.0	–0.9	+0.2	0.0
CWa	+2.5	+5.1	+14.5	0.0	0.0	+0.9	0.0
CWb	+33.7	+27.7	+21.9	0.0	+15.2	+0.7	0.0
CF	–6.1	–0.5	+14.1	–1.3	2.1	–1.3	0.0
CFa	–1.1	+7.1	+5.5	–1.3	+9.1	+3.1	0.0
CFb	+4.1	–4.1	+1.1	–1.1	–1.8	+11.8	0.0
DC	–13.2	–23.5	0.0	–35.6	–14.5	0.0	0.0
DCs	–15.1	–8.9	0.0	–46.8	–16.5	0.0	0.0
DCsa	–13.2	–20.3	–9.9	–12.2	–8.9	–13.5	0.0
DCsb	–12.2	–2.3	+0.9	–11.3	–11.4	–33.4	0.0
DCwa	–5.5	–2.2	–25.5	–5.5	–21.1	–20.7	0.0
DCwb	–44.5	–33.4	–45.2	–4.7	–26.5	–45.5	0.0
DCf	–5.6	–1.0	–0.1	–4.9	–15.5	0.0	0.0
DCfa	–9.2	–8.8	–23.2	–7.8	–18.8	0.0	0.0
DCfb	–11.3	–9.2	+0.2	–31.1	–16.4	0.0	0.0
E	–11.2	–20.2	0.0	–67.7	–14.5	0.0	–6.5
Ft	–18.8	–17.8	–4.5	–25.5	–20.4	0.0	–5.5
Fi	–20.1	–16.1	–17.7	–35.6	–21.1	0.0	–8.1

In Europe with the T increase by 2.5°C, i.e. 4.3°C, the climate types BS and BSh and their territories will increase by 19.3%, whereas DCS climate type will lose 1.4% of its territory (see [Figures 2 and 5](#)).

South America will have an increase of 65.6% of territories under Am climate type if global T increases by 4.3°C. The increase of average T between 0.3° and 4.3°C at a global scale in all analysed periods has greater effects on the climate types CW, CWa, CWb, and CF, and their covered areas will increase by 122.3% ([Figures 2–5](#)).

If the average global temperature increases by 1.1°C, the territories of all climate types in the period 2021–2040 will increase by 1.9%, and by 2.7% in the period 2040–2061 with an increase of T by 2.3°C. If T increases by 3.1°C, the increase will be 4.1% in the period 2061–2080. In the case of a global T increase by 4.3°C, the territories will increase by 6.1% in the period 2081–2100. The most resistant territories are those with climate types Ft and Fi. In Asia, territories with Ar climate type will suffer the biggest changes (see [Figures 2–5](#)). Climate types that present the territory of the desert, i.e., BW and Bwh, will have the biggest increase.

As has previously been stated, Australia is an isolated continent that will suffer huge consequences of climate change, as has been shown in the predictions reported here. The greatest changes will occur in the territories under climate types Ar, Am and Aw, which will increase, whereas the territories under climate types DCsb, DCwa and DCwb will decrease. The territories with tropical climate in South America in the period 2021–2100 will increase by 31.2%.

In North America, the territories with sub-tropical climates will increase the most. In North America and Europe, climate types CFa and CFb will lose the biggest territories. The most interesting part of the research is the fact that, according to TWCC, Australia gets a new climate Ar, in the case of a global T increase by 4.3°C ([Figures 2–5](#), [Table 2](#) and [Appendix S1](#)).

6 | DISCUSSION

The main goal of this paper was to map TWCC with updated temperatures taken from the synthetic grid of climate predictions MIROC6 and IPSL-CM6A- LR. This paper may be useful for future adaptations to climate change. Four scenarios of T increase with unequal distributions of precipitation were taken into consideration. The extreme scenario was analysed in particular (New et al., 2007). Mapping climate, although with certain errors and limitations, may give

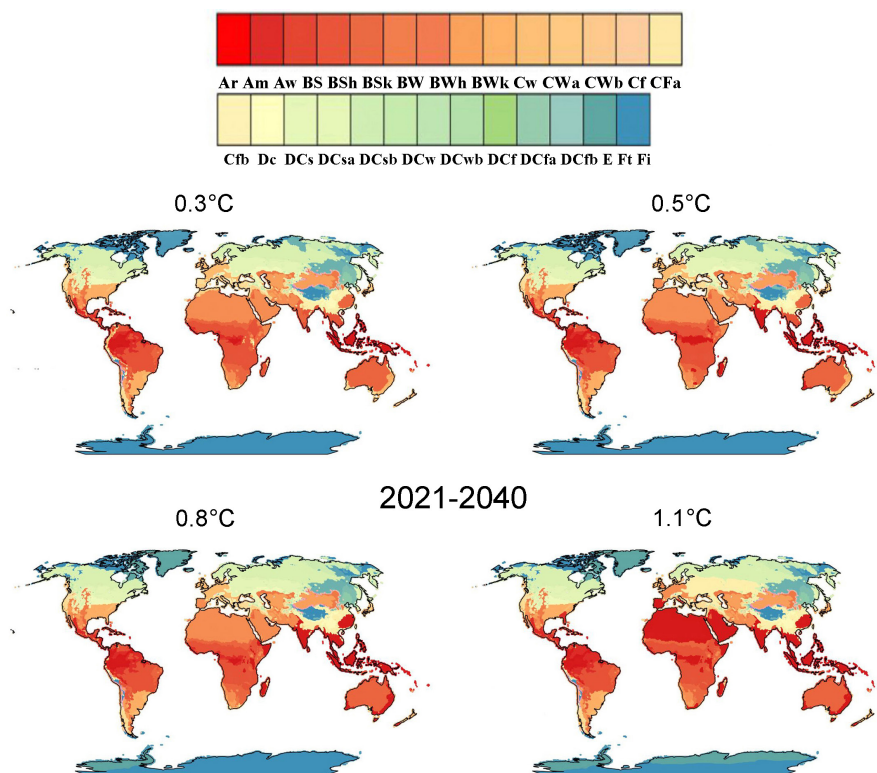


FIGURE 2 The territories of climate types according to TWCC in case of global T increase of 0.3°C, 0.5°C, 0.8°C and 1.1°C for the period 2021–2040

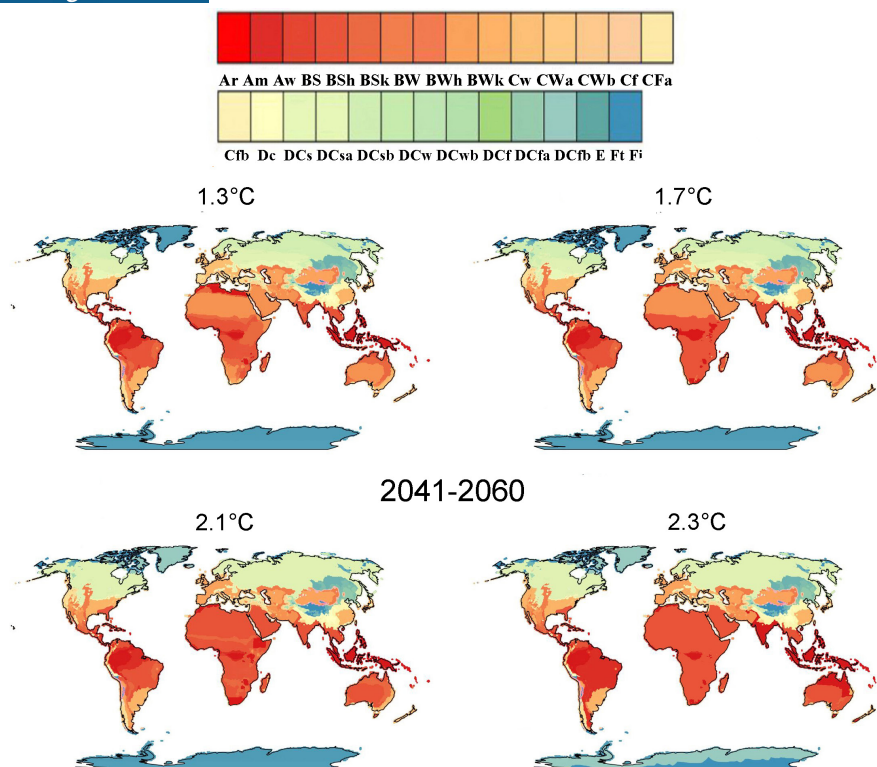


FIGURE 3 The territories of climate types according to TWCC in case of global T increase of 1.3°C, 1.7°C, 2.1°C and 2.3°C for the period 2041–2060

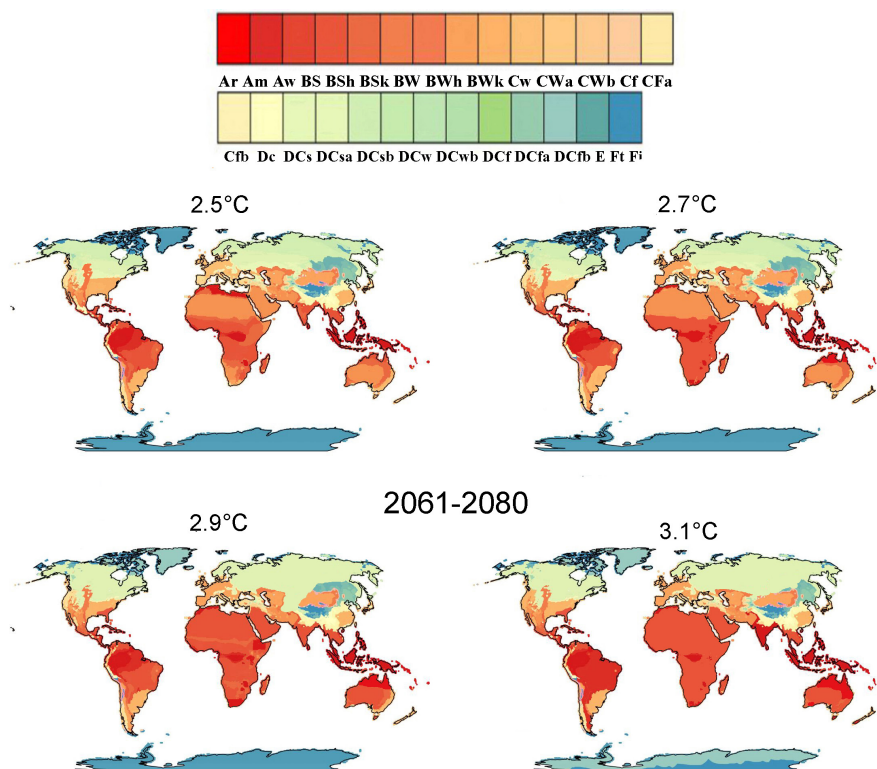


FIGURE 4 The territories of climate types according to TWCC in case of global T increase of 2.5°C, 2.7°C, 2.9°C and 3.1°C for the period 2061–2080

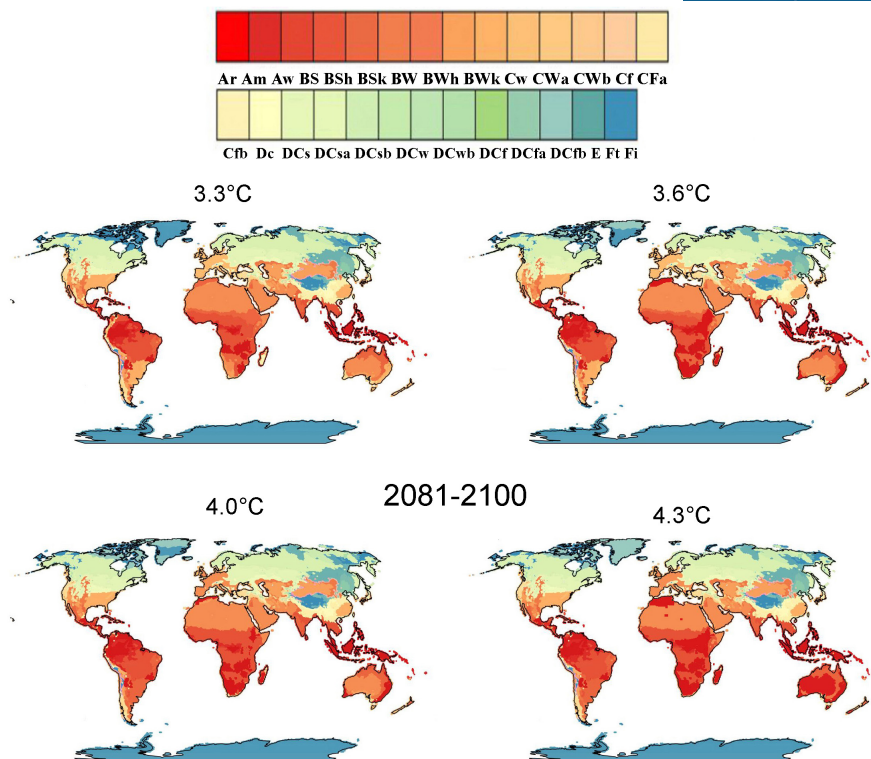


FIGURE 5 The territories of climate types according to TWCC in case of global T increase of 3.3°C, 3.6°C, 4.0°C and 4.3°C for the period 2081–2100

an indication of the change of climate types, as well as the biomes within these climates. The advantage of GIS and spatial analysis is the possibility to obtain the data on climate efficiently and rapidly. Visualisation aims to present all these changes in a more convenient way.

TWCC has not been used extensively in references worldwide, but this classification is suitable since it represents more sub-classes than the Köppen classification. Human activity has been the leading factor in the last century (Shine & Forster, 1999; Wang & Qin, 2017). In the Amazonian Basin, even a little increase in global temperature and a decrease in yearly precipitation may have consequences for forest distribution (Hulme & Turnpenny, 2004). Accordingly, the distribution of species cannot be the same as before (Li et al., 2000). Mapping climate types has a long history. There are numerous methods and climate classifications for mapping a climate property on a global scale. The Trewartha climate classification (TWCC) system, although very similar to Köppen-Geiger (KG), has some advantages. For example, the TWCC can present more differences between climate types within an area. Furthermore, the TWCC may be better at presenting local, regional and global scales of climate change effects (Klein et al., 2019). Finding the patterns of climate types and areas changing at a global scale has been an important task and the most significant question over the past decades. The current paper focuses on evaluating the global extent and distribution of updated climate types over a very long period that can help to improve our understanding of global change.

7 | CONCLUSIONS

The purpose of this research was to present updated global maps of TWCC. The grid taken for the purpose represents two climate models for the period between 2021 and 2100. Four potential scenarios of global temperature increase were used to model the change of amount of precipitation. All the data are in synthetic grids, out of which one was made using the advanced methodology of GIS. A total of 4261 control meteorological stations served to check the grid and distribution of climate. This classification, with its three predictions, may be a solid base for further, more detailed and more precise research on future climate changes. The paper focused on all the continents, including the Antarctic. Australia and Asia, South East Asia in particular, showed the biggest changes, whereas the Antarctic showed only minor changes. This may

also be encouraging, taking into account that the Antarctic would transform, and would disappear to a lesser extent, with a T increase by 4.3°C.

Overall, the following conclusions can be drawn:

1. Climate change impact on lands is a critical condition that affects the economy and future planning of living conditions on Earth; therefore, the TWCC should be preferred for climate change modelling applications.
2. It is found that, based on the new classification (i.e., TWCC), the impact of climatic change can modify the climate types, leading to an increase of up to 65.2% or a decrease to 39.1% and that this depends on the distribution of climate types.
3. The TWCC is designed to account for changes in land cover distribution and areas of urban and rural regions. Therefore, the use of TWCC for climate change impact studies can be powerful for representing realistic climate change impact on society.
4. Spatial analysis of climate belts, conducted in GIS, has shown that the biggest change in climate belts comes with the global temperature increase by 3.1°C. The biggest movement of climate belts which belong to A – tropical and B – dry climates is from the west to the east globally. Some future research on the same topic might present more climate classifications using the same climate data within the same period.

ACKNOWLEDGEMENTS

This research was supported by the H2020 WIDESPREAD-05-2020—Twinning: ExtremeClimTwin which has received funding from the European Union's Horizon 2020 research and innovation program under grant agreement No 952384. The authors acknowledge the support and constructive comments provided by Prof. Dr. Robert L. Wilby from the Department of Geography and Environment, Loughborough University, United Kingdom. The authors of this research are very grateful to the anonymous reviewers whose comments and suggestions significantly improved the overall quality of the manuscript.

DATA AVAILABILITY STATEMENT

The authors confirm that the data supporting the findings of this study are available within the article [and/or] its supplementary materials.

ORCID

Aleksandar Valjarević  <https://orcid.org/0000-0003-2997-2164>

REFERENCES

- Belda, M., Holtanová, E., Kalvová, J. & Halenka, T. (2016) Global warming-induced changes in climate zones based on CMIP5 projections. *Climate Research*, 71, 17–31. Available from: <https://doi.org/10.3354/cr01418>
- Comes, H.P. & Kadereit, J.W. (1998) The effect of Quaternary climatic changes on plant distribution and evolution. *Trends in Plant Science*, 3, 432–438. Available from: [https://doi.org/10.1016/S1360-1385\(98\)01327-2](https://doi.org/10.1016/S1360-1385(98)01327-2)
- Crowther, T.W., Glick, H.B., Covey, K.R., Bettigole, C., Maynard, D.S., Thomas, D.S. et al. (2015) Mapping tree density at a global scale. *Nature*, 525, 201–205. Available from: <https://doi.org/10.1038/nature14967>
- Daly, C., Gibson, W.P., Taylor, G.H., Johnson, G.L. & Pasteris, P. (2002) A knowledge-based approach to the statistical mapping of climate. *Climate Research*, 22, 99–113.
- De Castro, M., Gallardo, C., Jylha, K. & Tuomenvirta, H. (2007) The use of a climate type classification for assessing climate change effects in Europe from an ensemble of nine regional climate models. *Climate Change*, 81, 329–341.
- Feng, S., Ho, C., Hu, Q., Oglesby, R.J., Jeong, S.J. & Kim, B.M. (2012) Evaluating observed and projected future climate changes for the Arctic using the Köppen-Trewartha climate classification. *Climate Dynamics*, 38, 1359–1373. Available from: <https://doi.org/10.1007/s00382-011-1020-6>
- Fick, S.E. & Hijmans, R.J. (2017) Worldclim 2: New 1-km spatial resolution climate surfaces for global land areas. *International Journal of Climatology*, 37, 4302–4315. Available from: <https://doi.org/10.1002/joc.5086>
- Flannigan, M.D., Stocks, B.J. & Wotton, B.M. (2000) Climate change and forest fires. *Science of the Total Environment*, 262, 221–229. Available from: [https://doi.org/10.1016/S0048-9697\(00\)00524-6](https://doi.org/10.1016/S0048-9697(00)00524-6)
- Gotway, C.A., Ferguson, R.B., Hergert, G.W. & Peterson, T.A. (1996) Comparison of Kriging and inverse-distance methods for mapping soil parameters. *Soil Science Society of America*, 60, 1237–1247. Available from: <https://doi.org/10.2136/sssaj1996.03615995006000040040x>
- Govindasamy, B., Duffy, P.B. & Coquard, J. (2003) High-resolution simulations of global climate, part 2: Effects of increased greenhouse gases. *Climate Dynamics*, 21, 391–404.
- Hanberry, B.B. & Fraser, J.S. (2019) Visualizing current and future climate boundaries of the conterminous United States: Implications for forests. *Forests*, 10, 280. Available from: <https://doi.org/10.3390/f10030280>
- Hansen, M.C., Potapov, P.V., Moore, R., Hancher, M., Turubanova, S.A., Tyukavina, A. et al. (2013) High-resolution global maps of 21st-century forest cover change. *Science*, 342, 850–853. Available from: <https://doi.org/10.1126/science.1244693>

- Hijmans, R.J., Cameron, S.E., Parra, J.L., Jones, P.G. & Jarvis, A. (2005) Very high resolution interpolated climate surfaces for global land areas. *International Journal of Climatology*, 25, 1965–1978. Available from: <https://doi.org/10.1002/joc.1276>
- Hulme, M. & Turnpenny, J. (2004) Understanding and managing climate change: The UK experience. *Geographical Journal*, 170, 105–115. Available from: <https://doi.org/10.1111/j.0016-7398.2004.00112.x>
- Idso, S. & Brazel, A. (1984) Rising atmospheric carbon dioxide concentrations may increase streamflow. *Nature*, 312, 51–53. Available from: <https://doi.org/10.1038/312051a0>
- Keane, R.E., Holsinger, L.M. & Loehman, R.A. (2020) Bioclimatic modeling of potential vegetation types as an alternative to species distribution models for projecting plant species shifts under changing climates. *Forest Ecology and Management*, 477, 118498. Available from: <https://doi.org/10.1016/j.foreco.2020.118498>
- Klein, T., Cahanovitch, R., Sprintsins, M., Herr, N. & Schiller, G. (2019) A nation-wide analysis of tree mortality under climate change: Forest loss and its causes in Israel 1948–2017. *Forest Ecology and Management*, 432, 840–849. Available from: <https://doi.org/10.1016/j.foreco.2018.10.020>
- Köppen, W. (1923) *Die klimate der erde. Grundriss der klimakunde*. Berlin, Germany: Walter de Gruyter.
- Köppen, W. (1931) *Grundriss der klimakunde*. Berlin, Germany: Walter de Gruyter.
- Kotteck, M., Grieser, J., Beck, C., Rudolf, B. & Rubel, F. (2006) World map of the Köppen-Geiger climate classification updated. *Meteorologische Zeitschrift*, 15, 259–263. Available from: <https://doi.org/10.1127/0941-2948/2006/0130>
- Lai, Y.J., Tanaka, N., Im, S., Kuraji, K., Tantasirin, C., Tuankruea, V. et al. (2020) Climate classification of Asian university forests under current and future climate. *Journal of Forest Research*, 25, 136–146. Available from: <https://doi.org/10.1080/13416979.2020.1759898>
- Li, C., Flannigan, M.D. & Corns, I.G.W. (2000) Influence of potential climate change on forest landscape dynamics of west-central Alberta. *Canadian Journal of Forest Research*, 30, 1905–1912. Available from: <https://doi.org/10.1139/x00-118>
- Mwanukuzi, P.K. (2008) Using GIS for decision-making: The case of Kidunda dam in Morogoro, Tanzania. *Geographical Journal*, 174, 161–164. Available from: <https://doi.org/10.1111/j.1475-4959.2008.00288.x>
- New, M., Lopez, A., Dessai, S. & Wilby, R. (2007) Challenges in using probabilistic climate change information for impact assessments: An example from the water sector. *Philosophical Transactions of the Royal Society A*, 365, 2117–2131. Available from: <https://doi.org/10.1098/rsta.2007.2080>
- New, M., Lister, D., Hulme, M. & Makin, I. (2002) A high-resolution data set of surface climate over global land areas. *Climate Research*, 21, 1–25.
- North, P. (2013) Knowledge exchange, “impact” and engagement. *The Geographical Journal*, 179, 211–220. Available from: <https://doi.org/10.1111/j.1475-4959.2012.00488.x>
- Orus, R., Hernandez-Pajares, M., Juan, J.M. & Sanz, J. (2005) Improvement of global ionospheric VTEC maps by using kriging interpolation technique. *Journal of Atmospheric and Solar-Terrestrial Physics*, 67, 1598–1609. Available from: <https://doi.org/10.1016/j.jastp.2005.07.017>
- Peel, M.C., Finlayson, B.L. & McMahon, T.A. (2007) Updated world map of the Köppen-Geiger climate classification. *Hydrology and Earth System Sciences*, 11, 1633–1644. Available from: <https://doi.org/10.5194/hess-11-1633-2007>
- Prentice, C.I., Sykes, M.T. & Cramer, W. (1993) A simulation model for the transient effects of climate change on forest landscapes. *Ecological Modelling*, 65(1–2), 51–70. Available from: [https://doi.org/10.1016/0304-3800\(93\)90126-D](https://doi.org/10.1016/0304-3800(93)90126-D)
- Remedio, A.R., Teichmann, C., Buntemeyer, L., Sieck, K., Weber, T., Rechid, D. et al. (2019) Evaluation of new CORDEX simulations using an updated Köppen–Trewartha climate classification. *Atmosphere*, 10, 726. Available from: <https://doi.org/10.3390/atmos10110726>
- Richardson, M., Toigo, A. & Newman, C. (2007) Planet WRF: A general purpose, local to global numerical model for planetary atmospheric and climate dynamics. *Journal of Geophysical Research, Planets*, 112, 1–29.
- Robinson, S. (2020) Climate change adaptation in SIDS: A systematic review of the literature pre and post the IPCC Fifth Assessment Report. *WIREs Climate Change*, 11, e653. Available from: <https://doi.org/10.1002/wcc.653>
- Rohli, R.V., Joyner, A.T., Reynolds, S.J. & Ballinger, T.J. (2015) Overlap of global Köppen–Geiger climates, biomes, and soil orders. *Physical Geography*, 36, 158–175. Available from: <https://doi.org/10.1080/02723646.2015.1016384>
- Rohli, R.V. & Vega, A.J. (2012) *Climatology*, 2nd edition. Mississauga, ON: Jones and Bartlett Learning.
- Shakun, J., Clark, P., He, F., Marcott, S., Mix, A., Liu, Z. et al. (2012) Global warming preceded by increasing carbon dioxide concentrations during the last deglaciation. *Nature*, 484, 49–54. Available from: <https://doi.org/10.1038/nature10915>
- Shine, P.K. & Forster, F.M.P. (1999) The effect of human activity on radiative forcing of climate change: A review of recent developments. *Global and Planetary Change*, 20, 205–225. Available from: [https://doi.org/10.1016/S0921-8181\(99\)00017-X](https://doi.org/10.1016/S0921-8181(99)00017-X)
- Shiogama, H., Abe, M. & Tatebe, H. (2019) *MIROC MIROC6 model output prepared for CMIP6 ScenarioMIP ssp370. Version 20191114*. Earth System Grid Federation. <https://doi.org/10.22033/ESGF/CMIP6.5752>
- Smith, D.M., Cusack, S., Colman, A.W., Folland, C.K., Harris, G.R. & Murphy, J.M. (2007) Improved surface temperature prediction for the coming decade from a global climate model. *Science*, 317, 796–799. Available from: <https://doi.org/10.1126/science.1139540>
- Tatebe, H., Ogura, T., Nitta, T., Komuro, Y., Ogochi, K., Takemura, T. et al. (2019) Description and basic evaluation of simulated mean state, internal variability, and climate sensitivity in MIROC6. *Geoscientific Model Development*, 12, 2727–2765. Available from: <https://doi.org/10.5194/gmd-12-2727-2019>
- Thornton, M.W., Atkinson, P.M. & Holland, D.A. (2007) A linearised pixel-swapping method for mapping rural linear land cover features from fine spatial resolution remotely sensed imagery. *Computers and Geosciences*, 33, 1261–1272. Available from: <https://doi.org/10.1016/j.cageo.2007.05.010>

- Timpano, A.J., Zipper, C.E., Soucek, J. & Schoenholtz, D.J. (2011) Seasonal pattern of anthropogenic salinization in temperate forested head-water streams. *Water Research*, 133, 8–18. Available from: <https://doi.org/10.1016/j.watres.2018.01.012>
- Tokarska, K.B., Stople, M.B., Sippel, S., Fischer, E.M., Smith, C.J., Lehner, F. et al. (2020) Past warming trend constrains future warming in CMIP6 models. *Science Advances*, 6, eaaz9549. Available from: <https://doi.org/10.1126/sciadv.aaz9549>
- Valjarević, A., Djekić, T., Stevanović, V., Ivanović, R. & Jandžiković, B. (2018) GIS numerical and remote sensing analyses of forest changes in the Toplica region for the period of 1953–2013. *Applied Geography*, 92, 131–139. Available from: <https://doi.org/10.1016/j.apgeog.2018.01.016>
- Wang, Y. & Qin, D. (2017) Influence of climate change and human activity on water resources in arid region of Northwest China: An overview. *Advances in Climate Change Research*, 8, 268–278. Available from: <https://doi.org/10.1016/j.accre.2017.08.004>
- Wilby, R.L. & Wigley, T.M.L. (2002) Future changes in the distribution of daily precipitation totals across North America. *Geophysical Research Letters*, 29, 39-1–39-4. Available from: <https://doi.org/10.1029/2001GL013048>
- Zabel, F., Putzenlechner, B. & Mauser, W. (2014) Global agricultural land resources – a high resolution suitability evaluation and its perspectives until 2100 under climate change conditions. *PLoS One*, 9, e114980. Available from: <https://doi.org/10.1371/journal.pone.0114980>
- Zelinka, M.D., Myers, T.A., McCoy, D.T., Po-Chedley, S., Caldwell, P.M., Paulo, C. et al. (2020) Causes of higher climate sensitivity in CMIP6 models. *Geophysical Research Letters*, 47, e2019GL085782. Available from: <https://doi.org/10.1029/2019GL085782>

SUPPORTING INFORMATION

Additional supporting information can be found online in the Supporting Information section at the end of this article.

How to cite this article: Valjarević, A., Milanović, M., Gultepe, I., Filipović, D. & Lukić, T. (2022) Updated Trewartha climate classification with four climate change scenarios. *The Geographical Journal*, 00, 1–12. Available from: <https://doi.org/10.1111/geoj.12458>